

On Stability-Instability Analysis and an Optimal Linear Control to a Nonlinear Longitudinal Flight Dynamics

Danilo Carlos Pereira¹, José Manoel Balthazar², Fábio Roberto Chavarette³.

¹ Departamento de Projeto Mecânico, FEM, UNICAMP, 13083-970, Campinas, SP, Brasil, danilocp@pop.com.br

² Departamento de Estatística, Matemática Aplicada e Computação, IGCE, UNESP, 13506 – 700, Rio Claro, SP e professor visitante do Departamento de Projeto Mecânico, FEM, UNICAMP, 13083-970, Campinas, SP, jmbaltha@rc.unesp.br

³ Departamento de Estatística, Matemática Aplicada e Computação, IGCE, UNESP, 13506 – 700, Rio Claro, SP, fabioch@rc.unesp.br

Abstract: In this work, we analyzed the bifurcational behavior of a longitudinal flight nonlinear dynamics, taking as an example, the F-8 aircraft “Crusader”. We also studied the influence of the variation of the control parameters in its bifurcational behavior. We also presented results concerning to how much the aircraft’s mass variation, would may influence its dynamic behavior. Afterwards, we proposed a liner optimal control based, on nonlinear programming dynamics, applied to the considered nonlinear aircraft model. We also included high angles of attack, in order to stabilize the oscillations; those were close to the critical angle of the aircraft, in the flight conditions, established.

Keywords: Hopf Bifurcation, Stability, Nonlinear Flight Dynamics, Optimal Control Design. F8 Aircraft “Crusader”.

NOMENCLATURE

C_{L_w}, C_{L_t} = coefficients of wing and tail lift forces, respectively.

$C_{L_w}^i, C_{L_t}^i$ = coefficients of approximated wing and tail lift forces, respectively.

$c\dot{\theta}$ = damping moment.

g = gravitation Constant.

I_x, I_y, I_z = moments of inertia about axes x , y and z , respectively.

L_t, L_w = wing and tail lift forces, respectively.

l = distance between wing aerodynamic center (a.c) and aircraft’s center of gravity (c.g.).

l_t = distance between tail a.c. and aircraft’s c.g.

M_w = wing pitching moment.

m = mass of aircraft.

p, q, r = roll, pitch and yaw rates, respectively.

\bar{q} = dynamic pressure.

S = wing area.

S_t = horizontal tail area.

u, v, w = velocity components along x , y and z axes, respectively.

Greek Symbols

α = wing angle of attack.

α_t = tail angle of attack.

θ = pitch angle.

δ_e = deflection of elevator.

1. INTRODUCTION

There is not very much literature about nonlinear flight dynamics itself and most of it is quite old now. We mention, without deserve others; an excellent textbook that deals with nonlinear behavior in any significant way is that by (Pamadi, 2004). In terms of bifurcation analysis of nonlinear flight dynamics we may mention the work done by (Jahnke and Cullick, 1994). Note that much of the more recent works on nonlinear flight dynamics has focused on the analysis of the effects of specific non-linearities in the aircrafts with system of effective control. We are interest in a study of bifurcational analysis and in an application of an optimal linear control design problem to a longitudinal motion of an aircraft, taking into account of nonlinearities in aerodynamics and large amplitude motions, which typically occur during maneuvers, at high angles of attack approaching or exceeding the stalling angles. We remarked that although flights in high attack angles can bring an increase of significant agility, there is a great risk that a loss of stability it is happened, could suffer sudden transitions of stability and non-linearities(bifurcations).

Then, we study the nonlinear dynamics of a longitudinal flight, based on a mathematical model, which was proposed by Garrard and Jordan (Garrard, 1977). The used control parameters are: the deflection of the elevator and the mass of the considered aircraft. Taking into account the variation of these control parameters, it is looked for to identify and to describe the relationships between the behavior of the considered aircraft and the bifurcational phenomenon, exemplified, in the case of the aircraft F-8 “Cruzader”, that was proposed before by Liaw and Song (2001) and Liaw. We remarked that the results that we obtained here are in complete agreement with those results obtained, before, by Liaw, (2003). The adopted dynamic model of the aircraft is shown in the figure 1, with drag neglected; because it is considered to be small when it is compared to the lift force and weight of aircraft. The lift force was considered to be

separated into two components: in wing lift force and in tail lift force. Considering these suppositions, the governing equations of motion for longitudinal dynamics (with drag, no considered), are given by the equation (1. 1).

$$\begin{aligned}
 m(\dot{u} + w\dot{\theta}) &= -mg \sin \theta + L_w \sin \alpha + L_t \sin \alpha_i \\
 m(\dot{w} - u\dot{\theta}) &= mg \cos \theta - L_w \cos \alpha - L_t \cos \alpha_i \\
 I_y \ddot{\theta} &= M_w + lL_w \cos \alpha - l_t L_t \cos \alpha_i - c\dot{\theta}
 \end{aligned}
 \tag{1.1}$$

After some algebraic manipulation, we can obtain a fourth-order model of longitudinal dynamics with states (u, α, θ, q) and by considering that the aircraft flies in a constant velocity ($\dot{u} = 0$), we can reduce the mathematical model in a suitable form of three differential equations of third order, for the variables: (α : the attack angle; θ : the pitch angle and q : the pitch rate of the aircraft). In these considered equations: m denotes the mass of the aircraft and δ_e the control parameter, whose variation will make possible the study of possible bifurcations of the considered system. Assuming that the considered aircraft is in flight regime in a constant speed of $u=257,7 \text{ m/s}$ and, in an altitude of 9144 m (30.000 ft) and the initial mass m denoting by $m_0 = 9773 \text{ Kg}$, taking into account that $W := \{1/[1 + (\alpha/0.41)^{60}]\}$. We also assumed, for simplicity, that the moment of inertia I_y is to be proportional to the mass m . Then, the governing equations of motion may be written as:

$$\begin{aligned}
 \dot{\alpha} &= q \cos^2 \alpha + 0.0381 \cos^2 \alpha \cos \theta - (1/m)(564.434\alpha - 1693.301\alpha^3) \cos^3 \alpha W - \\
 &\quad (1/m)(35.145\alpha - 6.560\alpha^3 + 144.096\delta_e + 79.077\alpha^2\delta_e - 316.309\alpha\delta_e^2 - 421.745\delta_e^3) \times \cos^2 \alpha \\
 &\quad \cos(0.25\alpha + \delta_e) \\
 \dot{\theta} &= q \\
 \dot{q} &= -(1/m)264.409q + (1/m)(622.222\alpha - 1866.667\alpha^3) \cos \alpha W - (1/m)(3423.386\alpha - \\
 &\quad 641.885\alpha^3 + 14035.883\delta_e - 7702.619\alpha^2\delta_e - 30810.476\alpha\delta_e^2 - 41080.634\delta_e^3) \times \cos(0.25\alpha + \delta_e)
 \end{aligned}
 \tag{1.2}$$

We mention that we will organize this paper as follows. In Section 2, we do a stability-instability analysis outline of the solutions of the adopted governing equations of longitudinal motion of the aircraft F-8 ‘‘Crusader’’. In section 3 and 4 we present some numerical simulations carried out in the governing equations of motion. In section 5, we present an outline of a synthesis of an optimal control and, in Section 6 we present some examples of the application of this kind of control technique. In section7, we present the concluding remarks of this work, those presented here and in section 8, we do some acknowledgements. Finally, we list the main bibliographic used in this paper, in Section 9.

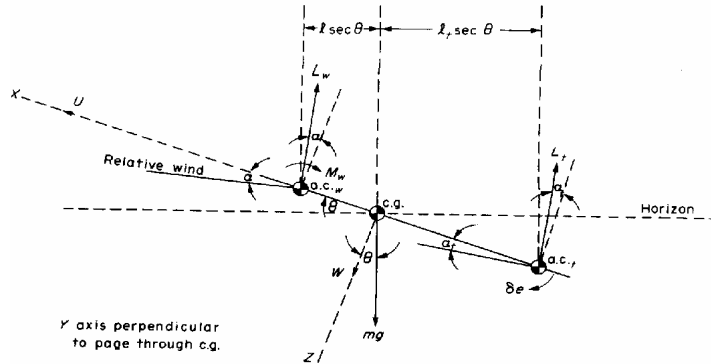


Figure 1: dynamic model of aircraft (Garrard, 1977).

2. STABILITY –INSTABILITY (BIFURCATIONAL) ANALYSIS OUTLINE.

Taking into account that the parameter $\delta_e \in (-0.2; 0)$ in (1.2), we carried out a number of numerical simulations. We remarked that the results, obtained here, are in complete agreement with those obtained, before by (Liaw and Song, 2001) and (Liaw; 2003). Here, we use the integrator ODE 45, of variable step length, and MATCONT®, a tool box of MATLAB® (Dhooge et al, 2003). This methodology is different of that used by (Liaw and Song, 2001) and (Liaw; 2003). Firstly, it is considered δ_e as a bifurcation parameter, with its variation in the interval $(-0.2; 0)$ and, it is chosen that the mass initial was $m=m_0$, where $m_0=9773 \text{ Kg}$. One observes that α should has a variation among 0 and $\pi/2$, because an aircraft easily cannot maintains a high angle of attack, during a considered flight. The equilibrium points of the equation (1.2) are analyzed and the eigenvalues in the equilibrium points of the associated Jacobian matrix of the dynamical system (1.2) is also evaluated. It is noticed that it presents: *two subcritical Hopf bifurcations and two saddle-node stationary bifurcations*. By using, the software MATCONT®, the stability of the equilibrium points of the system, are easily obtained, taking into account the governing equations of motion (1.2). It should be observed that the parameter α oscillates among 0 and $\pi/2$ (excluded the points in that $\alpha > \pi/2$). We obtained the numerical values those are presented in the table 1.

Table 1: Bifurcation Points (BP) for $m=m_0$.

B.P.	δ_e (rad)	α (rad)	θ (rad)	q (rad/s)
Hopf 1	-0,1058	0,4347	1,4588	0,0
Hopf 2	-0,1062	0,4360	-1,4773	0,0
SN 1	-0,0090	0,0448	0,0	0,0
SN 2	-0,0999	0,4177	0,0	0,0

Next, we obtain the bifurcation diagrams: In the figures 2 and 3, they show the equilibrium points and, the periodic solutions those emerge from the bifurcation points, taking into account the variation of the control parameter δ_e in the interval $[-0,2; 0]$. From the qualitative analysis of the figures 1 and 1, some observations can be inferred: The equilibrium point doesn't exist among two points limit, that is, for $\delta_e \in (-0, 0999; -0, 0090)$. The equilibrium points for α and q when $\theta < 0$ are the same as those for $\theta > 0$, but with reverse stabilities. It can also be visualized through the figure 3, the existence of a transition jump in the interval $\delta_e = (-0,099;-0, 0090)$, where the equilibrium of the dynamical system disappears. We remarked that, in the considered longitudinal dynamics, a jump means that the, θ and q states are divergent, in the discontinuous area of the system equilibria. And this characteristic also refers to the possibility to the stall phenomenon, which possibly implicates that the states of the system exhibit a jump in the flight dynamics of the aircraft. Figure 2 shows the property that the angle of attack is limited around $0, 01$ rad and that the aircraft, can loses stability, according to the deflection δ_e of the elevator, which varies when one maintains a high attack angle. Through the numeric simulations carried out, made further on. It is verified that the attack angle can be increased without it happens loss of the stability with the variation of the angle δ_e and also of the mass m of the aircraft.

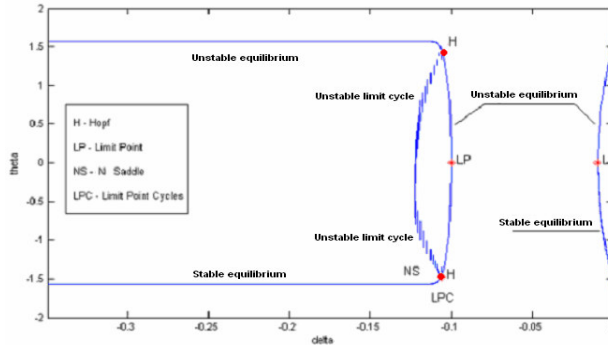


Figure 2: Equilibrium and periodic solutions for the system (1.2), $m=m_0$ in the variable q , with com $\theta < 0$ and $\theta > 0$.

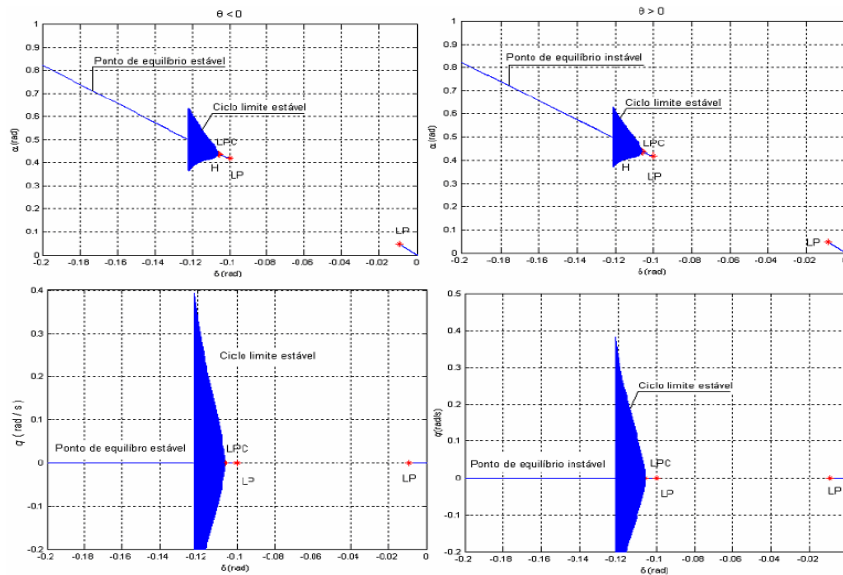


Figure 3: Equilibrium and periodic solutions for the system (1.2), $m=m_0$ in the variable q , with com $\theta < 0$ and $\theta > 0$.

3. TIME HISTORIES AND PHASE PORTRAIT PLANS TAKEN INTO ACCOUNT THE VALUES OF δ_e THOSE ARE GIVEN (IN TABLE 1).

In this section, it is observed, the topological behavior of the phase plan portrait, in one moment immediately previous and subsequent one, to the instant of the occurrence of the bifurcation. One knows that, when there is a bifurcation phenomenon, it is possible to obtain a qualitative change in the phase portrait of the considered dynamical system. Next, the behavior of the dynamical system equilibrium, will be analyzed, when the control parameter δ_e is varied. Then, taking into account the initial conditions of occurrence of Hopf bifurcation (See table 1) we will obtain the time history of the motion, and the evolution of the phase portrait plan, for each point of the table 1(with the objective of noticing a qualitative change in this considered phase plan).

In the figure 4, it is noticed a qualitative change in the phase portrait, that is obtained, when the parameter δ_e goes to the point, where a Hopf bifurcation happened.

In the figure 5, it is noticed the existence of a qualitative change in the phase portrait diagram, when the control parameter δ_e goes to the point, where will happens the Hopf bifurcation. It will be on the point Hopf 2, that it was given in the table 1. The qualitative change in the phase portrait is a property of a presence of a bifurcation.

In the figure 6, comes the evolution of the phase plan ($\alpha \times q$) according to the variation of δ_e directly to the point that happened a Saddle-Node bifurcation 1 (SN 1), showed by table 1. We can note a qualitative change in the phase portrait, as the parameter δ_e it goes by the point where happens to the bifurcation.

In the figure 7, it is presented the evolution of the phase plan ($\alpha \times q$), where it is being considered by taking the variation of δ_e for the (SN 2) point that is done in table 1. We also noticed the qualitative change in the phase portrait when the parameter δ_e , it goes to the point where happens the bifurcation.

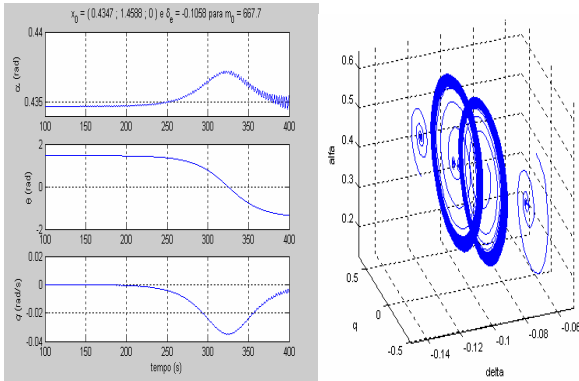


Figure 4: Historical of time and evolution of the phase plan with δ_e varying around the value regarding the point Hopf 1 of the table 1

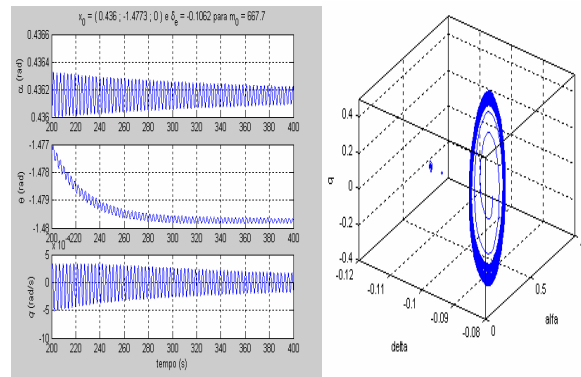


Figure 5: Historical of time and evolution of the phase plan with δ_e varying around the point Hopf 2 of the table 1.

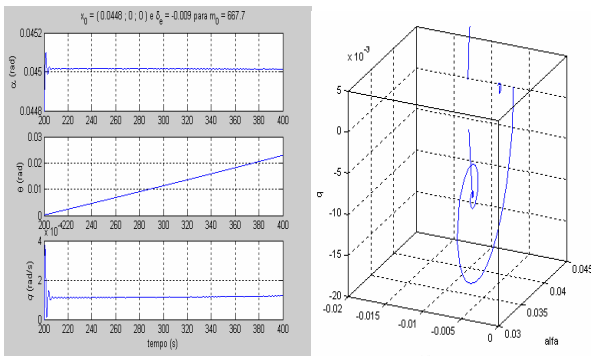


Figure 6: Historical of time and evolution of the phase plan with δ_e varying around the point Saddle 1 of the table 1.

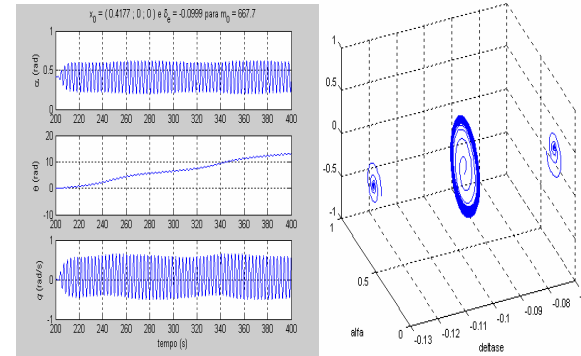


Figure 7: Historical of time and evolution of the phase plan with δ_e varying around the point Saddle-Node 2 of the table 1.

4. EFFECT OF THE AIRCRAFT MASS IN THE POINTS OF EQUILIBRIUM.

As one observes previously, there is a jump in the area of stability of the considered dynamical system. To solve this kind of problem, one may it is losing temper the mass m of the aircraft, what will affect, then, the existence of the equilibrium points. It should be observed that as we increased the mass of the aircraft, also increases the damping of the

system, as we assumed previously. In that way the mass m of the aircraft can be treated as a second bifurcation parameter.

After a number of numerical simulations, carried out, being taken different values of m , it is verified that are two limits points of the system those are more and more close to each other to measures that the mass is increased, until the moment in that the jump disappears. The figure 8 illustrates the behavior of the limits points as the mass is going increasing. As it was observed, not only the limits points are moved, but the bifurcation points are also rearranged. Besides, when the mass goes sufficiently big, two new bifurcation points will appear

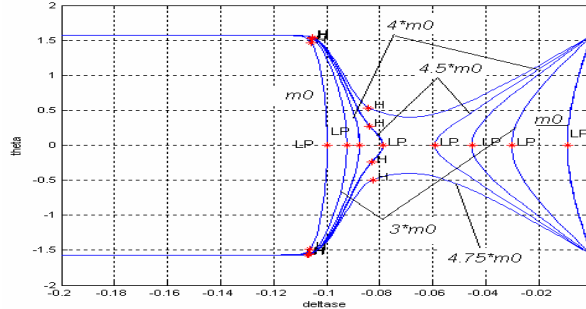


Figure 8: Evolution of the points limits in relation to the increase of the mass m_0 of the system.

In the figures 9, 10 and 11 are observed the evolution of the left limit point (LP). It is noticed that as the mass is increased two new points of Hopf bifurcation (H) close to the limit point (LP) they appear.

In the figure 11, it is shown the bifurcation diagram for the condition $m=4.47*m_0$. In this diagram are observed two equal Hopf bifurcations and a duplication of limits cycle that, in one on the sides it becomes stable. According to the value of the mass m increases, the left limit point (LP) becomes a bifurcation point type saddle-node for values of $m>4.35$.

Being made $m=4.58*m_0$, it is obtained a new diagram, as illustrated in the figure 12. It is interesting to notice that, although still there be a discontinuity in the interval of δ_ϵ , a stable cycle limit crosses this equilibrium points discontinuity when the mass $m=4.58*m_0$.

This fact can supply a solution to connect the jump behavior between both left and right bifurcation saddle-node points as δ_ϵ varies. In such a case, can the angle of attack be altered moving the value of δ_ϵ , but however it must notice that there aren't no stable equilibrium points between both points Hopf for negative pitch angles θ . Really, because as δ_ϵ it is going decreasing from the zero, the states firstly stay in stable equilibrium points, and then it jumps for a stable limit cycle when δ_ϵ to cross the first critical value in which happens the bifurcation.

According to the parameter δ_ϵ it continues to decrease of value, the oscillation of the system goes to δ_ϵ to cross the second critical point. When this fact happens, the states will converge again for a stable equilibrium, and then the attack angle can be increased efficiently through the control of the deflection of δ_ϵ .

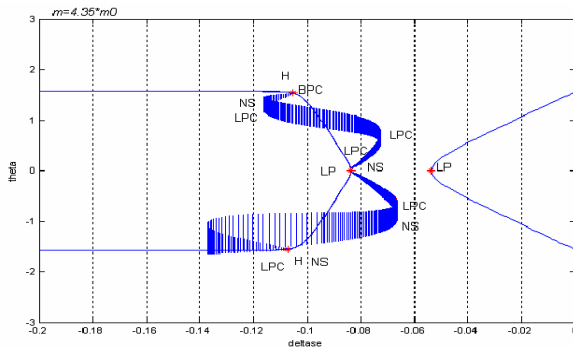


Figure 9: Evolution of the points limits in relation to the increase of the mass $=4.35m_0$.

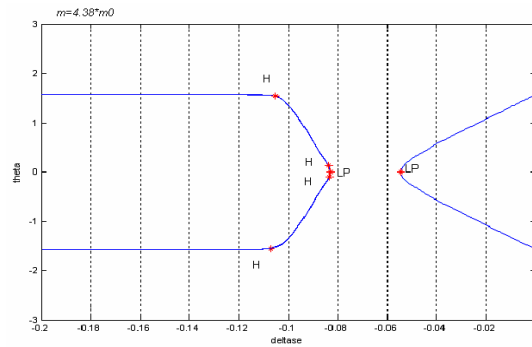


Figure 10: Evolution of the points limits in relation to the increase of the mass $=4.38m_0$.

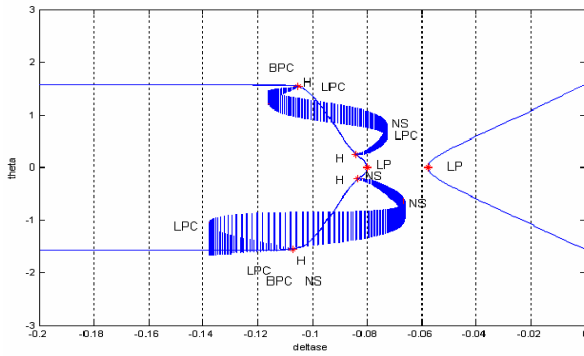


Figure 11: Evolution of the points limits in relation to the increase of the mass =4.47m₀.

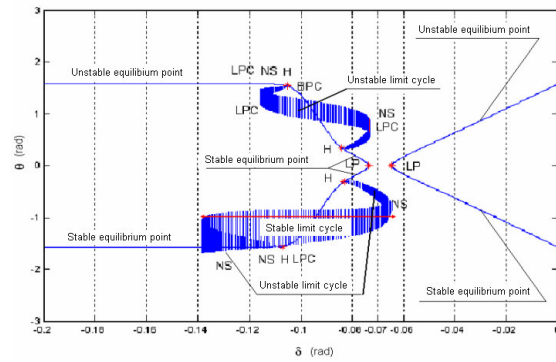


Figure 12: Evolution of the points limits in relation to the increase of the mass =4.58m₀.

The figures 13 and 14 show the time history for the system before and after the parameter δ_e to cross the saddle-node bifurcation point. In the figure 13 it is noticed that the system converges for a stable equilibrium point while, in the figure 14, the system converges for a stable limit cycle.

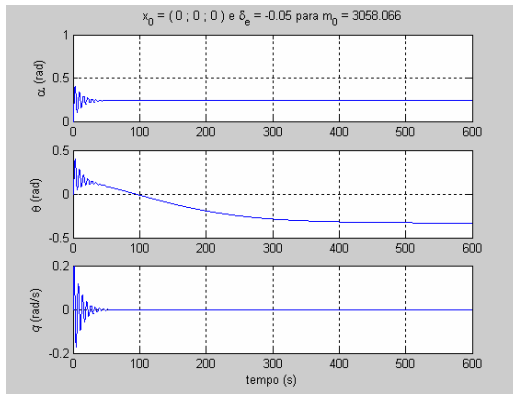


Figure 13: Time Historical in relation to the increase of the mass $m=4.58m_0$, with $\delta_e = -0.05$.

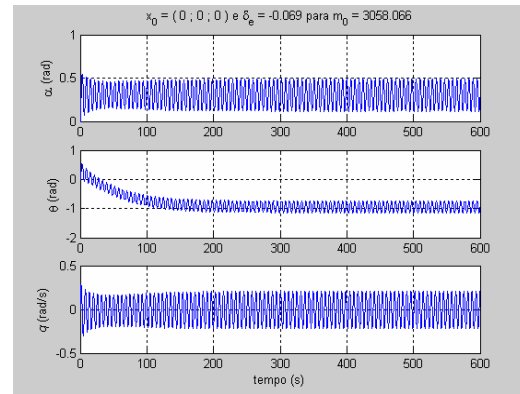


Figure 14: Time Historical in relation to the increase of the mass $m=4.58m_0$, with $\delta_e = -0.069$.

The figures 15 and 16 illustrate the system balance discontinuity disappearance when the mass parameter varies for $m=4.61*m_0$.

To analyze the qualitative behavior of the longitudinal dynamics of an aircraft, the characteristics and the existence of the equilibrium points are very important. In that way, it is verified that the increase of the mass m of the system (1.2) as, for example, for $m=5*m_0$, it takes the continuity of the equilibrium of the system for whole $\delta_e \in [-0.2; 0]$ as represented in the figure 16.

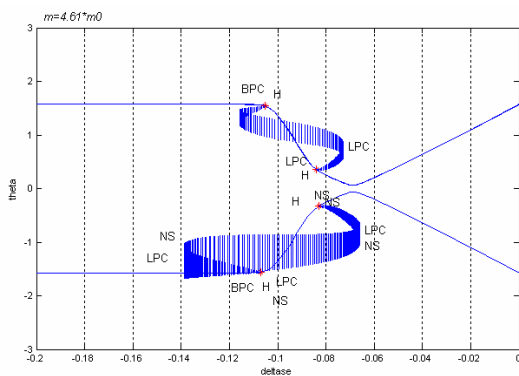


Figure 15: Evolution of the points limits in relation to the increase of the mass =4.61m₀.

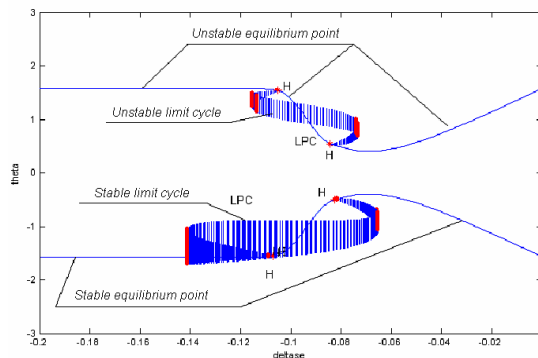


Figure 16: Balance and periodic solutions for the system with $m=5*m_0$.

One may observed, that the modified system has two equal of subcritical Hopf bifurcations. The locations of the bifurcations points are given in the table 2.

Additionally, in the figure 16, it had shown that the equilibrium points of the modified dynamical system.

We note that, with $m=5*m_0$ they are stable for $\theta < 0$, except for the points between Hopf bifurcations HPF-3 and HPF-4 given in y the table 2.

In the similar way, all of the equilibrium points are unstable for $\theta > 0$. Besides, the periodic solutions that emerge of the Hopf bifurcations HPF-3 and HPF-4 for $\theta < 0$ are observed as being stable limit cycles.

Table 2: Bifurcation Points (BP) for $m=5*m_0$.

B.P.	α (rad)	θ (rad)	q (rad)	δ_e (rad/s)
HPF-1	0.381108	0.531238	0	-0.084208
HPF-2	0.432570	1.541697	0	-0.105210
HPF-3	0.374950	-0.498879	0	-0.082545
HPF-4	0.439561	-1.559730	0	-0.107098

The time history and the evolutions of the phase portrait plans, for each point of the Hopf bifurcation of the table 2 are shown in the figures 17, 18 19 and 20.

In the evolution of the phase plan portraits, they are noticed those mentioned qualitative changes, as the parameter δ_e it goes by the point where happens the bifurcation (what it is a characteristic of bifurcation presence).

In next section, we will apply a synthesis of an optimal control to the considered problem. Taking into account an optimal control design, that as developed by (Rafikov and Balthazar, 2005, 2006).

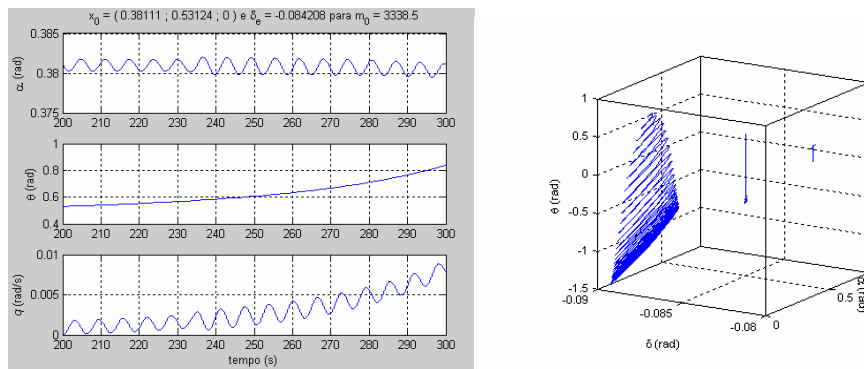


Figure 17: Historical of time and the evolution of the phase plan $\theta \times \alpha$ for the system (1.2) with $m=5*m_0$ and initial conditions for the point HPF-1 of the table 2.

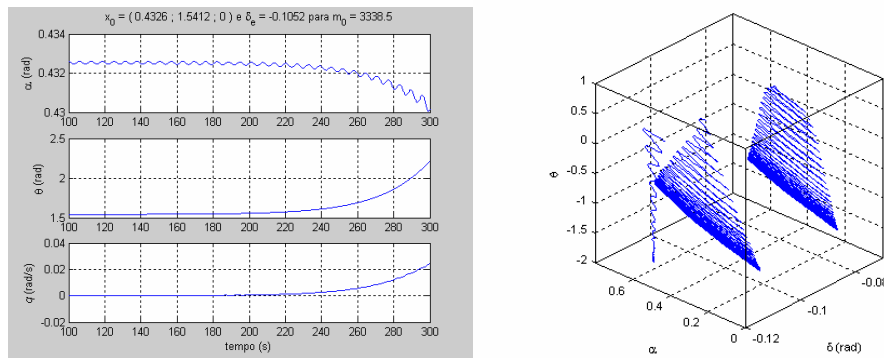


Figure18: Historical of time and the evolution of the phase plan $\theta \times \alpha$ for the system (1.2) with $m=5*m_0$ and initial conditions for the point HPF-2 of the table 2.

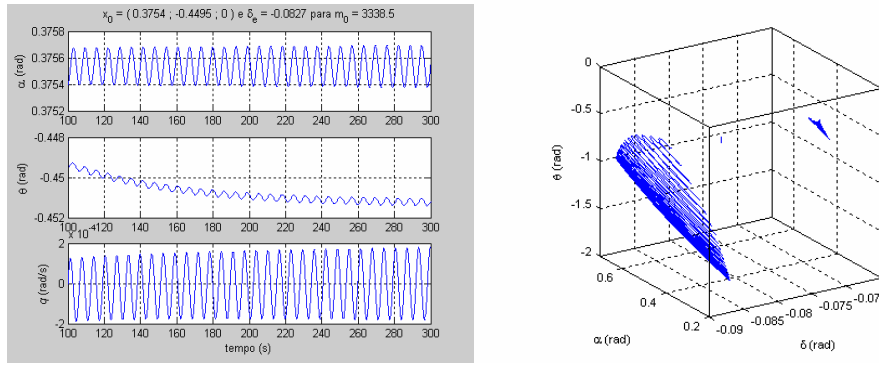


Figure 19: Historical of time and the evolution of the phase plan $\theta \times \alpha$ for the system (1.2) with $m=5*m_0$ and initial conditions for the point HPF-3 of the table 2.

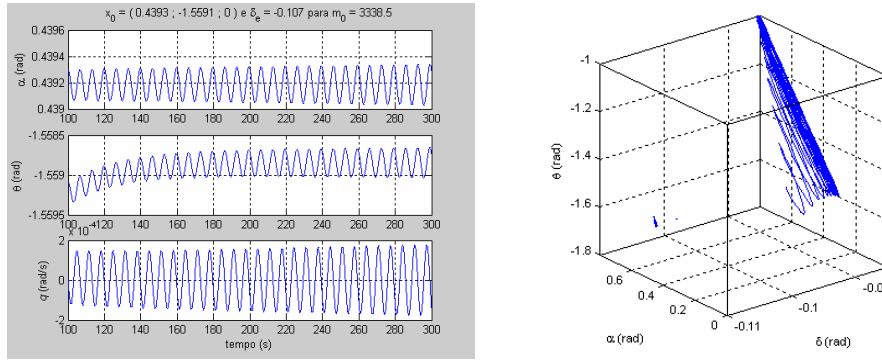


Figure 20: Historical of time and the evolution of the phase plan $\alpha \times \theta$ for the system (1.2) with $m=5*m_0$ and initial conditions for HPF-4.

5. OUTLINE OF A OPTIMAL CONTROL DESIGN

Due to the simplicity in the configuration and in the implementation, the linear state feedback control, is especially attractive (See, for instances (Rafikov, Balthazar, 2005, 2006)). We remarked that this approach is analytically, without dropping any non-linear term. Let the nonlinear governing equations of motion (1.1), those re-written in a state form (not unique)

$$\dot{x} = A(t)x + g(x) + U \quad (5.1)$$

If one considers a vector function \tilde{x} , that characterizes the desired trajectory, and taken the control U vector consisting of two parts: \tilde{u} being the feed forward and u_f is a linear feedback, in such way that

$$u_f = Bu \quad (5.2)$$

where B is a constant matrix. Next, one taking the deviation of the trajectory of system (5.1) to the desired one (5.1) $y = x - \tilde{x}$, written as

$$\dot{y} = Ay + G(x, \tilde{x})y + Bu \quad (5.3)$$

where $G(y, \tilde{x})$ is a limited matrix we proved the important result (Rafikov, Balthazar, 2005, 2006): If there exist matrixes $Q(t)$ and $R(t)$, positive definite, being Q symmetric, such that the matrix $\tilde{Q} = Q - G^T(y, \tilde{x})P(t) - P(t)G(y, \tilde{x})$ is positive definite for the limited matrix G , then the linear feedback control

$$u = -R^{-1}B^T P(t) y \quad (5.4)$$

is optimal, in order to transfer the non-linear system (5.2) from any initial to final state $y(t_f) = 0$, minimizing the functional $J = \int_0^{t_f} (y^T \tilde{Q} y + u^T R u) dt$, where the symmetric matrix $P(t)$ is evaluated through the solution of the matrix Ricatti differential equation

$$\dot{P} + PA + A^T P - PBR^{-1}B^T P + Q = 0 \quad (5.5)$$

Satisfying the final condition $P(t_f) = 0$.

6. LINEAR DESIGN FOR LONGITUDINAL NONLINEAR DYNAMICS

Next, we show, some few examples of the application of the above control technique, by considering two particular cases, those were discussed above (see tables 1 and 2). An extension to another's cases, it will be easy done, in similar way. Firstly, taking into account the initial conditions: $m=9773Kg$; $\alpha=0.4 \text{ rad}$; $\theta=-1.5 \text{ rad}$; $q=0.1 \text{ rad/s}$ e $\delta_e=-0.11$, where there is a Hopf bifurcation (Pereira, Balthazar, 2006) and will obtain:

$$B = \begin{bmatrix} 1 \\ 0 \\ 0 \end{bmatrix}, y = \begin{bmatrix} x_1 - \tilde{x}_1 \\ x_2 - \tilde{x}_2 \\ x_3 - \tilde{x}_3 \end{bmatrix}, \tilde{x} = \begin{bmatrix} 0 \\ 0 \\ 0 \end{bmatrix}, Q = \begin{bmatrix} 0.25 & 0 & 0 \\ 0 & 0.25 & 0 \\ 0 & 0 & 0.25 \end{bmatrix}, A = \begin{bmatrix} -0.6003 & 0.9714 & 0 \\ -4.2266 & -0.3960 & 0 \\ 0 & 1 & 0 \end{bmatrix} \quad (6.1)$$

where $M = |B| |AB| |A^2B| \neq 0$ (the considered dynamical system is controllable). Then the Matrix P (t) is done by

$$P = \begin{bmatrix} 0.3993 & -0.0682 & -0.2500 \\ -0.0682 & 0.0551 & 0.0591 \\ -0.2500 & 0.0591 & 0.2833 \end{bmatrix} \text{ and (an optimal control) } u = 0.9531x_1 - 0.2133x_2 - 0.5x_3. \quad (6.2)$$

The figure 21 shows the results with control and without control. In this illustration it can be observed that the aircraft is submitted to a high angle of attack of 22.92° (0.4 rad) and we remarked that this angle are very close to the value I (criticize of stall for the aircraft in the flight conditions established). As mentioned in Garrard (1977) the aircraft in flight in a speed of 257.7 m/s and in 9773 m of altitude, it has an angle of stall of 23.5° (0.4102 rad). In that way the controller is observed that it stabilized the attack angle that, for the authors, it was satisfactory.

Secondly, taking into account, the initial conditions, to occurrence of Saddle Node Bifurcation (Pereira, Balthazar, 2006) $m=9773Kg$; $\alpha=0.4360 \text{ rad}$; $\theta=0 \text{ rad}$; $q=0 \text{ rad/s}$ e $\delta_e=-0.1062$, choosing the same matrixes (B, y, \tilde{y}, Q) done by (6.1), we will obtain

$$A = \begin{bmatrix} -0.0153 & 0.8108 & 0 \\ -5.2015 & -0.3960 & 0 \\ 0 & 1 & 0 \end{bmatrix}, P = \begin{bmatrix} 0.7128 & -0.0449 & -0.2500 \\ -0.0449 & 0.0728 & 0.0350 \\ -0.2500 & 0.0350 & 0.2278 \end{bmatrix}, u = 1.5271x_1 - 0.2046x_2 - 0.5x_3. \quad (6.3)$$

The figure 22 shows the results with control and without control. In this illustration it can be observed that the aircraft is submitted to a high angle of attack of 24.981° (larger than the critical angle of stall) and, in that way it is observed that the controller stabilized the attack angle, showing a satisfactory result.

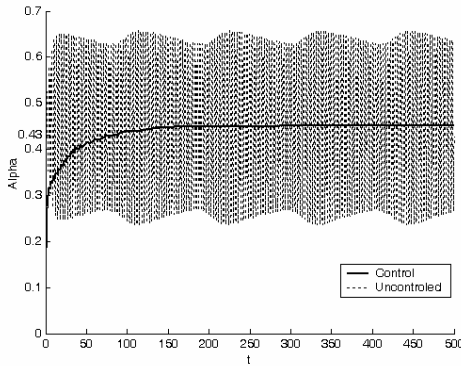


Figure 21: Historical of time taking $m=9773Kg$; $\alpha=0.4 \text{ rad}$; $\theta=-1.5 \text{ rad}$; $q=0.1 \text{ rad/s}$ e $\delta_e=-0.11$.

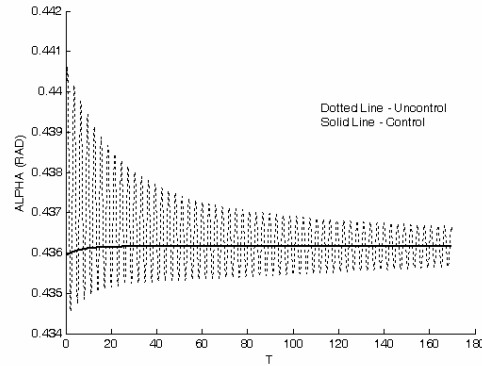


Figure 22: Historical of time taking $m=9773Kg$; $\alpha=0.4360 \text{ rad}$; $\theta=0 \text{ rad}$; $q=0 \text{ rad/s}$ e $\delta_e=-0.1062$.

7. CONCLUSIONS

In this work, we did a study of the stability and the behavior of the non linear dynamics of longitudinal flight. We were taking into consideration the data of aircraft F-8 "Crusader" that was discussed, before, in (Garrard, 1977). The bifurcational behavior of the dynamics of longitudinal flight was investigated, taking into account two control parameters: firstly, with respect to the deflection δ_e of the elevator and later in relation to the variation of the mass m of the aircraft.

Here, we reproduce the results those were obtained before, but here, we used different methodology. We also investigated the behavior of the dynamic behavior before and after the occurrence of bifurcation, in order to understand better the involved phenomena. In the numeric simulations, which were carried out, here, the numerical integrator ODE 45 of variable steplenght **MATLAB**[®] was used. We also use a “toolbox” of **MATCONT-MATLAB**[®].

The results those were obtained before were some bifurcations of saddle-node and Hopf kind. The occurrence of bifurcations saddle-node and Hopf they can result in jump behaviors and pitch oscillations. Those jumps can provoke a discontinuity in the equilibrium of the system, and this region where exists a discontinuity can possibly mean, according in Liaw and Song (2001), that the aircraft is trying to get STALL situations.

Those bifurcations can contribute to sudden behaviors of jumps in the pitch dynamics of the aircraft. It is ended, also that the control parameter m , used in this study as being the mass of the aircraft, it can play an important part in the longitudinal flight dynamics. Such results can be very important for the project of aircrafts, when the mass change becomes significant.

We applied a synthesis of an optimal control design to some cases of the considered problem, which theory was recently developed by (Rafikov and Balthazar, 2005, 2006). We remarked that this technique is based on analytical solutions and works without dropping any important contributions those are present in the governing equation of motion.

We remarked that an extension to all cases of numerical values done by Tables 1 and 2, are easily done. They were published, on separately. Note that the results presented, here, have a strong indicative that this kind of optimal control design can lead a significant improvement in considered aircraft. Extension to another aircrafts will be easily done.

Future works will complete the dynamic and control analysis that we was stared here, in order to provide a dynamical response over the entire range of angle of attack because a modern high performance aircraft may operate, avoiding hazardous flying qualities.

The study of the interaction between the longitudinal and lateral motion of the considered aircraft for high angle of attack will be also considered, as a challenge in next papers, by using the same methodology, discussed in this paper.

8. ACKNOWLEDGMENTS

The first author thanks FAPESP and the second author thanks to FAPESP and CNPq both Brazilian Researches Funding Agencies.

9. REFERENCES

- Dhooge, A., Govaerts, W., Kuznetsov Y. A., 2003. “Matcont: A Matlab Package for Numerical Bifurcation Analysis of Odes”, ACM TOMS 29(2), pp. 141 – 164.
- Garrard, W.L.; Jordan, J.M.; 1977. “Design of Nonlinear Automatic Flight Control Systems”. Automatica, vol. 13, nº 5, pp. 497 – 505. Pergamon Press.
- Jahnke CC, Culliak, FEC, [1994] Application of Bifurcation Theory to the High –Angle-of- Attack Dynamics of the F-14, Journal of Aircraft, Vol. 31, N1, 26-34, 1994
- Liaw, D-C.; Song, C-C.; 2001. “Analysis of Longitudinal Flight Dynamics: A Bifurcation-Theoretic Approach”. Journal of Guidance, Control and Dynamics. Vol. 24, nº 1, pp. 109 – 116, January – February.
- Liaw, D-C.; 2003. “Two-Parameter Bifurcation Analysis of Longitudinal Flight Dynamics”. IEEE Transactions on Aerospace and Electronic Systems, vol. 39, nº 3, pp 1103 – 1110, July.
- Pamadi B; 2004, “Performance, Stability Dynamics & Control of Airplanes, AIAA, © 2004, 2nd Edition, 780 pages.
- Pereira, D.C.; Balthazar, J.M.; *Sobre A Dinâmica Não-linear de uma Aeronave em Vôo Longitudinal* – Proceedings of IV Congresso Nacional de Engenharia Mecânica, Recife - PE, Brasil, august 22-25, 2006. In Portuguese. CD-ROM, 2006.
- Rafikov, M, Balthazar, J, M. Optimal Linear and Nonlinear Control Design for Chaotic Systems. DETC2005-84998. Proceedings of IDETC’05, 2005 ASME International Design Engineering Technical Conferences and Computers and Information in Engineering Conference Long Beach, California, USA, September 24–28, 2005, CD ROM, 2005.
- Rafikov, M, Balthazar, J, M. Optimal Linear Control Design for Nonlinear Systems. Journal of Computational and Nonlinear Dynamics, ASME, USA, Submitted, 2006.

10. RESPONSIBILITY NOTICE

The author(s) is (are) the only responsible for the printed material included in this paper.